PRAMANA
— journal of
physics

Vol. 60, No. 5
May 2003
pp. 877–885

Intriguing aspects in baryon production at relativistic heavy-ion collider

HUAN ZHONG HUANG
Department of Physics and Astronomy, University of California at Los Angeles, Los Angeles, CA 90095-1547, USA

Abstract. We review experimental results on baryon production at mid-rapidity in nucleus–nucleus collisions at RHIC. Outstanding physics issues include the mechanism for baryon–anti-baryon production from thermally equilibrated partons, the dynamics of baryon number transport and the evolution dynamics of baryons during hadronic expansion before the final freeze-out. We highlight recent measurements on the production of protons, lambdas and their anti-particles in terms of these physics issues. We propose a physical mechanism of topological baryon formation through gluon junction hadronization and future measurements, which can test this hypothesis experimentally.

Keywords. Baryon; hyperon; heavy-ion collisions.

PACS No. 25.75.Dw

1. Introduction

The commencement of the relativistic heavy ion collider (RHIC) operation at Brookhaven National Laboratory (BNL) has ushered in a new era for the study of quantum chromodynamics (QCD) at extremely high-energy density and temperature. Initial results indicate that an unprecedented high-energy density has been achieved in nucleus–nucleus collisions in the laboratory [1–3]. A large anisotropy, the elliptic flow parameter v_2, has also been observed indicating that the initial anisotropy in the geometrical overlap of the colliding nuclei leads to a large anisotropy of particle emission in the final state momentum distribution [4]. The measured ratio of $\bar{p}$ to p, ~ 0.65, is considerably larger than the ratios at previous facilities for heavy-ion collisions [5–7]. This large $\bar{p}/p$ ratio at RHIC is consistent with the interaction picture that the net baryon density at mid-rapidity in Au + Au collisions at RHIC ($\sqrt{s_{NN}} = 130$ GeV) is small. The baryon pair production contributes to the total baryon yield significantly, relative to baryon number transport. Thus, nuclear matter formed at mid-rapidity in nucleus–nucleus collisions at RHIC is of extreme high-energy density with small finite net baryon numbers.

Baryons including high mass hyperons are unique probes for nuclear collision dynamics [8–11]. Outstanding questions include: (1) mechanisms for baryon production from a thermalized quark–gluon plasma (QGP); (2) dynamics for baryon number transport from the colliding nuclei to mid-rapidity and (3) evolution of baryons during the expansion after the initial colliding stage. In this talk I highlight features of baryon production at mid-rapidity from Au + Au collisions at $\sqrt{s_{NN}} = 130$ GeV using mostly data from the STAR

experiment. The measurements are compared with expectations from string fragmentation models for baryon production. A new novel mechanism is proposed to explain the increased yield of high mass hyperons and future measurements, which can be used to test this mechanism.

2. Experimental features of baryon production at RHIC

The solenoidal tracker at RHIC (STAR) experiment is one of the major experiments at RHIC. The central detector during the summer 2000 run is a large time projection chamber (TPC) inside a solenoidal magnet operating at 0.25 T field. The TPC provides both tracking for charged particles and measurement of ionization energy loss (dE/dx) for limited particle identification with 2π azimuthal coverage. Two zero-degree calorimeters (ZDC) measure neutrons along the direction of the colliding beams and provide a minimum bias interaction trigger. A central trigger barrel (CTB) made of scintillating paddles surrounding the TPC outer field cage provides a central interaction trigger. Details of the detector configuration and data analyses have been described elsewhere [12,13].

_Figures 1 and 2 show the transverse mass (m_T) spectra of anti-proton ($\bar{p}$) and anti-lambda (Λ) for several centrality bins, where the collision centrality is defined offline using reconstructed TPC tracks as described in refs [3,14,15]. The $\bar{p}$ sample is selected using

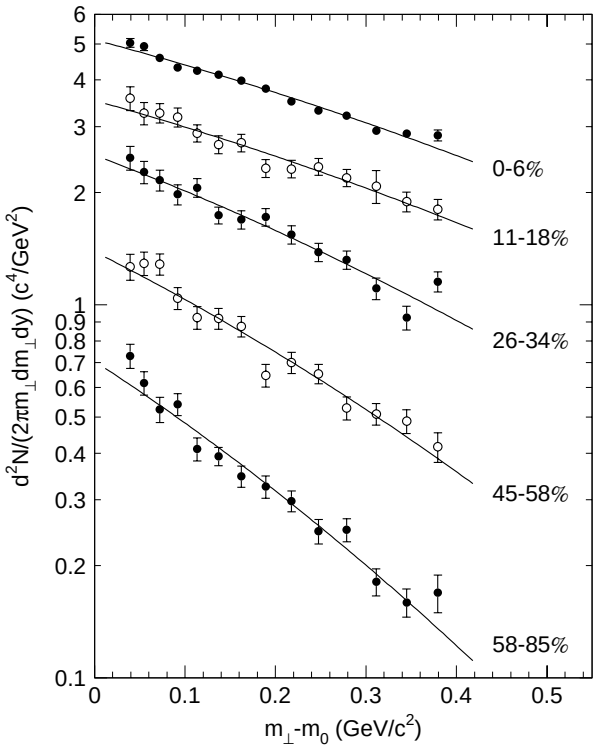

Figure 1. Transverse mass distributions of $\bar{p}$ for selected centrality bins. The dashed lines are Gaussian p_T fits.

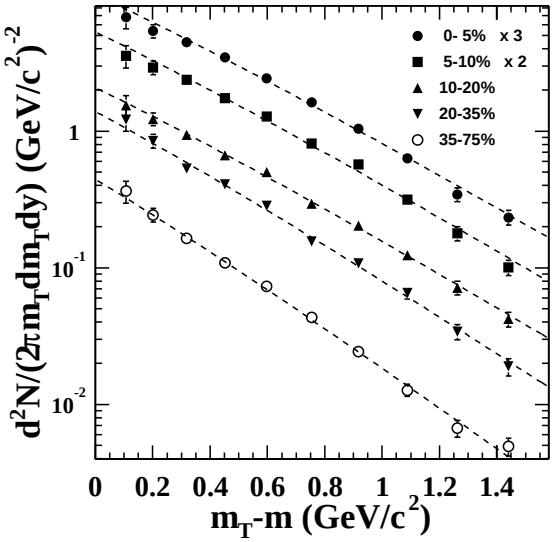

Figure 2. Transverse mass distributions of $\bar{\Lambda}$ for selected centrality bins. The dashed lines are the Boltzmann fits.

dE/dx from the TPC and is restricted to transverse momentum $p_T < 1$ GeV/c. The $\bar{\Lambda}$ sample is from reconstruction of its topological decay, $\bar{\Lambda} \to \bar{p} + \pi^+$. The limited m_T region for the $\bar{p}$ spectra allows for fit functions of exponential m_T, Boltzmann and Gaussian p_T. The extrapolated rapidity density dn/dy over the whole p_T region varies over 25% when these functions are used. However, by comparing the functional extrapolations to high p_T outside the $\bar{p}$ identification region with the measured p_T spectra of negatively charged hadrons (h^-) [14], it was determined that the Gaussian p_T distribution provided extrapolations matching the h^- measurement best in the high p_T region. The resultant $\bar{p}$ dn/dy for the most central (5%) collisions is 20.5 ± 0.5. The PHENIX experiment reported a $\bar{p}$ dn/dy of 20.1 ± 1.0 from a class of events with similar centrality [16,17].

The p_T range for the $\bar{\Lambda}$ spectra is much broader. Both exponential m_T and Boltzmann distributions provide reasonable fits to the $\bar{\Lambda}$ data. The Boltzmann fit generally has a slightly better χ^2 per degree of freedom and gives a reasonable fit of the m_T spectra over the entire range of centrality and p_T coverage. The total dn/dy from these two functional fits are consistent with each other within the statistical uncertainties. The measured $\bar{\Lambda}$ yield in the TPC acceptance is over 70% of the total dn/dy. For the most central collisions the measured dn/dy for Λ and $\bar{\Lambda}$ are $17.0 \pm 0.4(\text{stat.}) \pm 1.8(\text{syst.})$ and $12.0 \pm 0.3(\text{stat.}) \pm 1.3(\text{syst.})$, respectively. The feed-down contribution to the $\Lambda(\bar{\Lambda})$ dn/dy from decays of multiply-strange hyperons is estimated to be about $(27 \pm 6)\%$ of the measured yields [15].

The shapes of the m_T spectra for $\bar{p}$ and $\bar{\Lambda}$ depend strongly on collision centralities. The yield from peripheral collisions falls much more steeply as a function of m_T than that from central collisions. This trend is more prominent in the $\bar{p}$ spectra which cover a low p_T region. Figure 3 shows the slope parameters from the Boltzmann m_T fits as a function of h^-, where h^- is the average number of negatively charged hadrons within pseudorapidity $|\eta| < 0.5$ from events of the selected centrality bins in figures 1 and 2. The slope

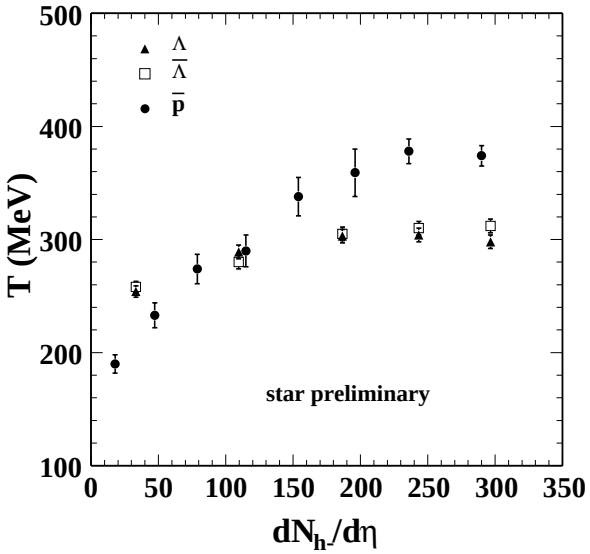

Figure 3. The slope parameters of $\bar{p}$, $\bar{\Lambda}$ and Λ from Boltzmann fits as a function of negative hadron multiplicity density at mid-rapidity. Errors shown are statistical only.

parameters increase as a function of h^-: approximately 260 MeV from the peripheral to 300 MeV from the central collisions for Λ and $\bar{\Lambda}$. The slope parameters of $\bar{p}$ are sensitive to the p_T range: the PHENIX experiment reported a slope parameter of $\bar{p}$ similar to the STAR slope parameters for Λ and $\bar{\Lambda}$ for central collisions when the covered p_T range is approximately the same. The large slope parameters for $\bar{p}$ measured in the STAR TPC are likely due to the very limited p_T coverage for particle identification based on dE/dx.

Figure 4 shows the baryon rapidity density as a function of h^-, where the errors are statistical only. The production rates of $\bar{p}$, Λ and $\bar{\Lambda}$ are approximately proportional to the h^- yield. The lines are the results of linear fits. The Λ/h^- and $\bar{\Lambda}/h^-$ ratios are 5.4% and 4.0%, respectively, independent of the collision centrality. The linear fit does not work well for the $\bar{p}$ yield. The $\bar{p}$ yield in central collisions is above the linear fit. However, the systematic errors for the m_T integrated $\bar{p}$ yield, where about 70% of the yield comes from extrapolations outside the measured m_T region, are much larger than Λ and $\bar{\Lambda}$.

Figure 5 shows the baryon dn/dy as a function of h^- from HIJING [18], where the mechanism for baryon production is the LUND string fragmentation model as implemented in JETSET [19,20]. The production rate of baryons in HIJING is also proportional to the number of negative hadrons. However, the coefficients for the proportionality are very different. HIJING produces too many $\bar{p}$, and the anti-baryon to baryon ratios, $\bar{p}/p$ and $\bar{\Lambda}/\Lambda$, are higher than the STAR measurement. There is an approximate agreement in the Λ yield between HIJING and the STAR measurement if we take into account the feed-down contribution from Ξ hyperons in the STAR Λ yield [15]. Because the difference in the $\bar{p}$ yield between HIJING and the STAR measurement is so large, this approximate agreement in the Λ yield may be a coincidence.

Figure 6 shows the $\bar{p}/h^-$ and $\bar{\Lambda}/h^-$ ratios as a function of p_T from the most central collisions (5%). The ratios increase with p_T very rapidly. This trend is consistent with the

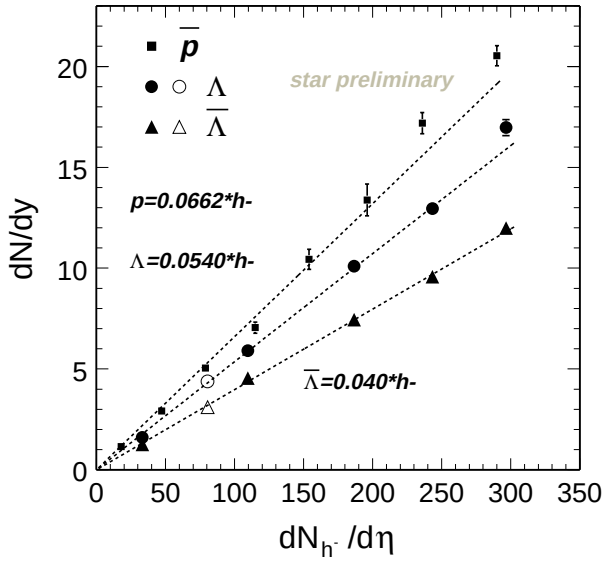

Figure 4. The rapidity density of $\bar{p}$, $\bar{\Lambda}$ and Λ as a function of negative hadron multiplicity density at mid-rapidity. The lines are the results of linear fits: $y = ax$.

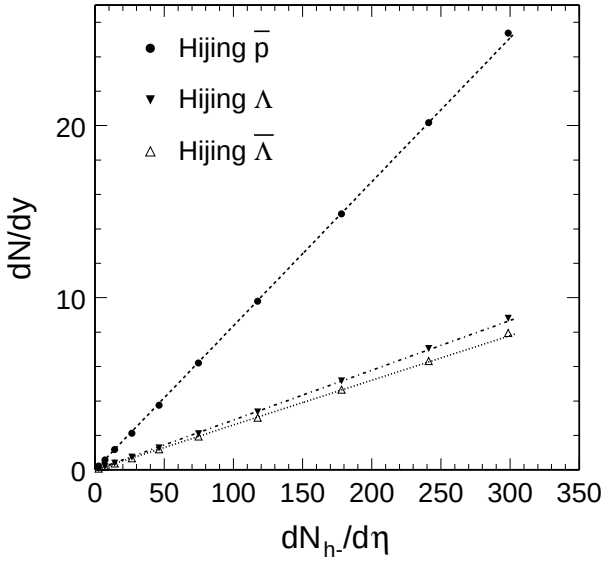

Figure 5. The HIJING rapidity density of $\bar{p}$, $\bar{\Lambda}$ and Λ as a function of negative hadron multiplicity density at mid-rapidity.

fact that the slope parameters for baryons are considerably higher than those for mesons. However, the actual magnitude of this ratio is surprising. For example, the $\bar{\Lambda}/h^-$ ratio

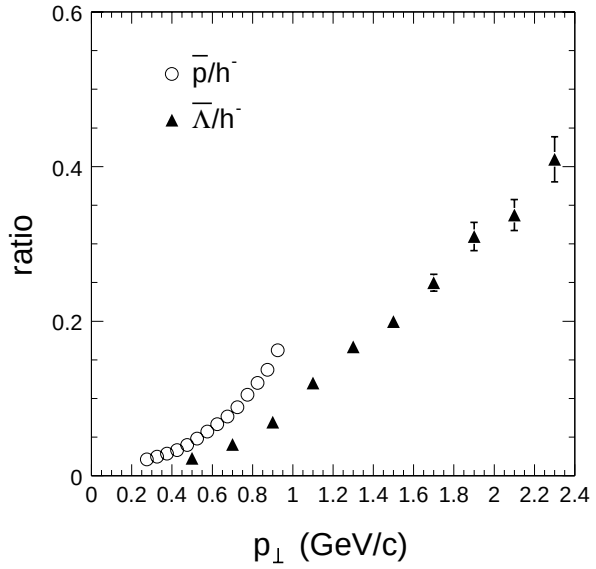

Figure 6. The $\bar{p}/h^-$ and $\bar{\Lambda}/h^-$ ratios as a function of p_{T} from the central (5%) collisions.

is about 0.35 at $p_{\mathrm{T}} = 2.0$ GeV/c. This large ratio is consistent with the observation by PHENIX [17,21] that the $\bar{p}/\pi^-$ ratio approaches 1 at p_{T} of 2.0 GeV/c, which corresponds to a $\bar{p}/h^-$ ratio slightly below 0.5.

As shown in figure 5, HIJING over-predicts the total yield of $\bar{p}$. However, the HIJING pseudo-rapidity density of charged particles is close to the RHIC measurement [1,3]. The $\bar{p}/h^-$ ratio from HIJING at moderate p_{T} of 2.0 GeV/c is approximately 0.2, much less than the experimental value close to 0.5. HIJING with and without jet quenching does not change the ratio as a function of p_{T} significantly. The comparison between HIJING and the STAR data seems to indicate that HIJING produces too many $\bar{p}$ and the p_{T} distribution of $\bar{p}$ falls too steeply. The final state interaction among produced hadrons, which is missing in HIJING, can in principle increase the average p_{T} of particles, baryons in particular, and will flatten the baryon p_{T} distribution. However, it is also possible that new underlying baryon production dynamics may be responsible for the increased yield of baryons at high p_{T} whereas the current string fragmentation scheme in HIJING fails to describe features of the baryon production.

3. Novel mechanism for baryon formation

Our comparison of baryon production between HIJING and the STAR data indicates that HIJING significantly over-predicts the total number of $\bar{p}$. The discrepancies in Λ and $\bar{\Lambda}$ yields between HIJING and the STAR data are smaller. Therefore, the total production rate of baryons in nucleus–nucleus collisions at RHIC is not a limiting factor in the string fragmentation model. However, the theoretical mass-flavor dependence of the baryon production rate is drastically wrong. In the Lund string fragmentation model [19], baryons

are produced via the production of di-quark pairs by quantum tunneling from string potential and subsequent hadronization of the di-quarks into baryons. The tunneling probability depends on $e^{-\pi m^2/\kappa}$, where m is the di-quark mass and κ is the string tension. This mass dependence severely limits the production rate of strange di-quarks. For multiply-strange baryons, the production rate for the extra strange quark is further suppressed compared to light quarks. This dynamical production mechanism, when it is applied to baryon production from ultra-relativistic heavy-ion collisions, does not seem to yield a balanced distribution of protons and hyperons that matches experimental data. Modification schemes of the string fragmentation model, for example, color string ropes [22] and string fusion [23], have very limited success in enhancing high mass hyperon yields. The deficiency can be attributed to the exponential m^2 dependence intrinsic in string fragmentation models.

We propose a baryon formation mechanism based on the gluon junction configuration existing in the baryon wave function. The gluon junction is a topological configuration arising from gauge invariance where schematically three gluon strings are connected together to a junction at one end while the other end is connected to valance quarks [24]. The interaction of the gluon junction in nuclear collisions has been applied to baryon number transport dynamics [10] and baryon pair productions [25]. The latter was developed in the framework of string fragmentation dynamics. Our basic assumptions are:

1. High density gluon matter is formed at mid-rapidity in nucleus–nucleus collisions at RHIC. The partonic dynamics are dominated by strongly interacting gluons which may be produced from the initial gluon structure function of the colliding nuclei.
2. The gluon junction, i.e., three gluons connected with each other to a single joint, should be a natural topological configuration in the strongly interacting gluon fields. This gluon junction can be a seed for dynamically creating a baryon number.
3. The gluon string may break into quark and anti-quark pairs and a baryon (anti-baryon) is generated when three gluon strings all combine with a quark (anti-quark) in hadronization process. The flavor of the baryon is determined by the flavor of the quarks connected to the gluon junction. The mass of the baryon originates mostly from the gluon junction.
4. The rate of baryon production depends on the topological configuration probability of the gluon junctions and the subsequent hadronization scheme. The process is expected to be non-perturbative QCD in nature.

Two predictions on baryon yields can be made from the topological formation model through gluon junctions:

$$\bar{\Lambda}^0 = \bar{\Sigma}^0 = \bar{\Sigma}^+ = \bar{\Sigma}^-, \quad \bar{\Xi}^0 = \bar{\Xi}^+ \tag{1}$$

and

$$\frac{\bar{\Lambda}^0}{\bar{p}} = \frac{\bar{\Xi}^+}{\Lambda^0} = \frac{\bar{\Xi}^0}{\Lambda^0} = \alpha \geq \frac{\bar{\Omega}^+}{\Xi^+}. \tag{2}$$

The $\bar{\Omega}$ production could be different because it belongs to baryon decuplet with different internal structure from the others which belong to baryon octet. We apply this novel baryon formation mechanism to the $\bar{p}$ and $\bar{\Lambda}$ data from the STAR collaboration at RHIC [14,15]:

$$20.5 \pm 0.5 = \bar{p} + 0.64(\bar{\Lambda}^0 + \bar{\Sigma}^0 + \bar{\Xi}^0 + \bar{\Xi}^+ + \bar{\Omega}^+) + 0.52\bar{\Sigma}^+, \tag{3}$$

$$8.8 \pm 0.9 = \bar{\Lambda}^0 + \bar{\Sigma}^0, \tag{4}$$

where all yields are primary and the feed-down correction factor has been applied to the measured hyperon yield. Solving these two equations for α parameter we obtained a value of approximately 0.6–0.7. The resultant primordial baryon yields for $\alpha \sim 0.62$ are: $\bar{p} = 7.6$; $\Lambda^0 = \bar{\Sigma}^0 = 4.6$; $\bar{\Xi}^0 = \bar{\Xi}^+ = 3$ and $\bar{\Omega}^+ \leq 1.8$.

In the gluon junction topological mechanism for the formation of baryons the slope parameters of all baryons, $\bar{p}$, Λ, $\bar{\Xi}$ and $\bar{\Omega}$, should be very close to each other, to the first order, regardless of their masses and hadronic cross-sections with the medium. The apparent large slope parameters are mostly due to the kinematic distribution of topological gluon junctions at the hadronization epoch. We also note that the STAR measurement indicates that the slope parameters of Λ and $\bar{\Lambda}$ are the same within statistical uncertainties, even though the production mechanisms may differ: the $\bar{\Lambda}$s are primarily pair produced while approximately 30% of the Λs carry baryon number from the colliding nuclei. The exact dynamics that dictate the same slope parameters for these hyperons and anti-hyperons have not been established yet. The gluon junction interaction has been previously proposed as the mechanism to transport baryon number over a large rapidity gap [10], in which case the dynamics for the hyperon and anti-hyperon production can be similar, leading to comparable m_{T} distributions.

4. Future perspective

We have presented salient features in baryon production from Au + Au collisions at RHIC for $\sqrt{s_{NN}} = 130$ GeV. String fragmentation models for baryon production through di-quark quantum tunneling out of the string potential do not have the correct mass dependence for proton and hyperon yields. We propose a dynamical baryon production picture through the hadronization of gluon junctions. The baryon production rate depends on the probability for the topological junction configuration in the high density gluonic fireball formed in nucleus–nucleus collisions. We predict similar yields for $\bar{\Lambda}$ and $\bar{\Sigma}^0$, and dn/dy for the $\bar{\Xi}$ and $\bar{\Omega}$ production of approximately 3 and $\sim$1–2, respectively. Future measurements of these hyperons will provide more insight into the dynamics of baryon production and test this novel baryon formation mechanism.

Acknowledgements

We thank the STAR collaboration, in particular, Yu Chen, Hui Long and An Tai, for providing the STAR data figures. We gratefully acknowledge the useful discussions with D Kharzeev, L McLerran and An Tai on the baryon formation mechanism proposed in this paper. We thank Steve Trentalange and Charles Whitten for the careful reading of the manuscript.

References

[1] B B Back *et al*, *Phys. Rev. Lett.* **85**, 3100 (2000)
[2] K Adcox *et al*, *Phys. Rev. Lett.* **86**, 3500 (2001)

[3] C Adler *et al*, *Phys. Rev. Lett.* **87**, 112303 (2001)
[4] K H Ackermann *et al*, *Phys. Rev. Lett.* **86**, 402 (2001)
[5] C Adler *et al*, *Phys. Rev. Lett.* **86**, 4778 (2001)
[6] B B Back *et al*, *Phys. Rev. Lett.* **87**, 102301 (2001)
[7] I G Bearden *et al*, *Phys. Rev. Lett.* **87**, 112305 (2001)
[8] J Ellis *et al*, *Phys. Lett.* **B233**, 223 (1989)
[9] W Busza and R Ledoux, *Ann. Rev. Nucl. Part. Sci.* **38**, 119 (1989)
[10] D Kharzeev, *Phys. Lett.* **B378**, 238 (1996)
[11] J Rafelski and B Muller, *Phys. Rev. Lett.* **48**, 1066 (1982); **56**, 2334(E) (1986)
[12] K H Ackermann *et al*, *Nucl. Phys.* **A661**, 681c (1999)
[13] H Caines for the STAR Collaboration, *Pramana – J. Phys.* **60**, 627 (2003)
[14] C Adler *et al*, STAR Collaboration, *Phys. Rev. Lett.* **87**, 262302 (2001)
[15] C Adler *et al*, STAR Collaboration, Mid-rapidity Λ and $\bar{\Lambda}$ production in Au + Au collisions at $\sqrt{s_{NN}} = 130$ GeV, submitted to *Phys. Rev. Lett.* (March 2002)
[16] K Adcox *et al*, submitted to *Phys. Rev. Lett.*, nucl-ex/0112006
[17] J Velkovska for the PHENIX Collaboration, *Pramana – J. Phys.* **60**, 1011 (2003)
[18] X N Wang, *Phys. Rep.* **280**, 287 (1997)
[19] B Andersson *et al*, *Phys. Scr.* **32**, 574 (1985)
[20] T Sjostrand, PYTHIA 5.7 and JETSET 7.4: Physics and Manual, hep-ph/9508391
[21] K Adcox *et al*, submitted to *Phys. Rev. Lett.*, nucl-ex/0201008
[22] H Sorge, *Phys. Rev.* **C52**, 3291 (1995)
[23] N Amelin *et al*, *Phys. Lett.* **B306**, 312 (1993)
[24] G C Rossi and G Veneziano, *Nucl. Phys.* **B123**, 507 (1977)
[25] S E Vance *et al*, *Phys. Lett.* **B443**, 45 (1998)